

## Discovery and In Vitro Optimization of 3-Sulfamoylbenzamides as ROMK Inhibitors

Matthew F. Sammons, Sujay V. Kharade, Kevin J. Filipski, Markus Boehm, Aaron C. Smith, Andre Shavnya, Dilinie P. Fernando, Matthew S. Dowling, Philip A Carpino, Neil A. Castle, Shannon G. Zellmer, Brett M. Antonio, James R. Gosset, Anthony Carlo, and Jerod S. Denton

ACS Med. Chem. Lett., **Just Accepted Manuscript** • DOI: 10.1021/acsmchemlett.7b00481 • Publication Date (Web): 19 Jan 2018

Downloaded from <http://pubs.acs.org> on January 21, 2018

### Just Accepted

“Just Accepted” manuscripts have been peer-reviewed and accepted for publication. They are posted online prior to technical editing, formatting for publication and author proofing. The American Chemical Society provides “Just Accepted” as a free service to the research community to expedite the dissemination of scientific material as soon as possible after acceptance. “Just Accepted” manuscripts appear in full in PDF format accompanied by an HTML abstract. “Just Accepted” manuscripts have been fully peer reviewed, but should not be considered the official version of record. They are accessible to all readers and citable by the Digital Object Identifier (DOI®). “Just Accepted” is an optional service offered to authors. Therefore, the “Just Accepted” Web site may not include all articles that will be published in the journal. After a manuscript is technically edited and formatted, it will be removed from the “Just Accepted” Web site and published as an ASAP article. Note that technical editing may introduce minor changes to the manuscript text and/or graphics which could affect content, and all legal disclaimers and ethical guidelines that apply to the journal pertain. ACS cannot be held responsible for errors or consequences arising from the use of information contained in these “Just Accepted” manuscripts.

# Discovery and In Vitro Optimization of 3-Sulfamoylbenzamides as ROMK Inhibitors

Matthew F. Sammons,<sup>\*,†</sup> Sujay V. Kharade,<sup>\*,#</sup> Kevin J. Filipowski,<sup>†</sup> Markus Boehm,<sup>†</sup> Aaron C. Smith,<sup>§</sup> Andre Shavnya,<sup>§</sup> Dilinie P. Fernando,<sup>§,‡</sup> Matthew S. Dowling,<sup>§</sup> Philip A. Carpino,<sup>†</sup> Neil A. Castle,<sup>°,‡</sup> Shannon G. Zellmer,<sup>°,‡</sup> Brett M. Antonio,<sup>°,‡</sup> James R. Gosset,<sup>†</sup> Anthony Carlo,<sup>§</sup> and Jerod S. Denton<sup>#</sup>

<sup>†</sup> Pfizer Worldwide Research & Development, 610 Main Street, Cambridge, MA 02139, United States

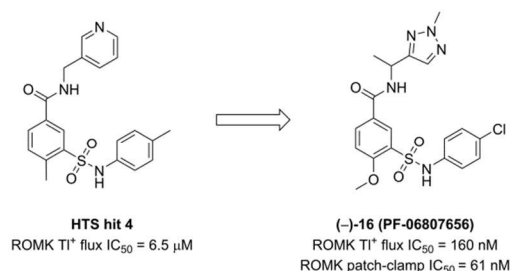
<sup>#</sup> Department of Anesthesiology, Vanderbilt University Medical Center, Nashville, TN 37232, United States

<sup>§</sup> Pfizer Worldwide Research & Development, Eastern Point Road, Groton, CT 06340, United States

<sup>°</sup> Neusentis, Pfizer Worldwide Research & Development, Durham, NC 27703, United States

**KEYWORDS:** ROMK, Kir1.1, potassium channel inhibitors, diuretics, hypertension

**ABSTRACT:** Inhibitors of the renal outer medullary potassium channel (ROMK) show promise as novel mechanism diuretics, with potentially lower risk of diuretic-induced hypokalemia relative to current thiazide and loop diuretics. Here we report the identification of a novel series of 3-sulfamoylbenzamide ROMK inhibitors. Starting from HTS hit **4**, this series was optimized to provide ROMK inhibitors with good in vitro potencies and well-balanced ADME profiles. In contrast to previously reported small-molecule ROMK inhibitors, members of this series were demonstrated to be highly selective for inhibition of human over rat ROMK and to be insensitive to the N171D pore mutation that abolishes inhibitory activity of previously reported ROMK inhibitors.



Diuretics are a cornerstone of current strategies for pharmacological treatment of hypertension and for reduction of edema and fluid retention associated with heart failure. Approximately 88% of patients hospitalized with acute decompensated heart failure receive intravenous loop diuretics.<sup>1</sup> Thiazide diuretics are recommended as first-line agents for the treatment of hypertension and are among the most prevalent antihypertensive agents used in the United States.<sup>2,3</sup> However, these agents are not without limitations. Both loop and thiazide diuretics are associated with metabolic imbalances, particularly low levels of blood potassium (hypokalemia).<sup>4</sup> Loop diuretics lose efficacy upon chronic administration and high doses may be required to achieve sufficient exposure at the site of action in patients with impaired renal function.<sup>5</sup> It is estimated that among adults in the U.S. approximately 6.5 million have heart failure, approximately 85 million are hypertensive, and the prevalence of both conditions is projected to increase in the coming decades.<sup>6</sup> There is thus an urgent need to develop novel mechanism of action pharmaceutical agents for the treatment of these conditions that lack the limitations of current diuretics.

The renal outer medullary potassium channel (ROMK, Kir1.1) plays a major role in renal salt handling and reabsorption,<sup>7</sup> and inhibitors of ROMK show promise as novel mechanism diuretic agents.<sup>8</sup> Potassium conductance via ROMK is required for both Na<sup>+</sup>/K<sup>+</sup>/2Cl<sup>-</sup> co-transporter (NKCC2)-

mediated salt absorption in the thick ascending limb of the Loop of Henle (TAL) and potassium excretion in the TAL and cortical collecting duct (CCD).<sup>9</sup> The first reported selective, small-molecule ROMK inhibitor VU591 (**1**, Figure 1) was demonstrated to inhibit potassium transport in isolated perfused rat collecting duct tubules with no effect on sodium transport.<sup>10</sup> Since this initial report, several disclosures by investigators at Merck<sup>11-19</sup> have established the in vivo efficacy of small-molecule ROMK inhibitors (Figure 1), including Compound A (**2**) and clinical candidate MK-7145 (**3**), as powerful diuretic and natriuretic agents that, in contrast to thiazides and loop diuretics, have minimal impact on kaliuresis.<sup>20-22</sup> A number of small-molecule ROMK inhibitors have also been disclosed in the patent literature.<sup>23</sup>

Herein, we report the discovery and in vitro optimization of a novel series of ROMK inhibitors based on a 3-sulfamoylbenzamide scaffold that shows remarkable species-selective inhibition and an insensitivity to mutations of the ROMK channel that ablate the inhibitory activity of other small-molecule ROMK inhibitors.

The Pfizer compound collection was screened for inhibitors of TI<sup>+</sup> uptake, a well-established surrogate for K<sup>+</sup> conductance in ion channels,<sup>24</sup> into HEK-293 cells expressing the short isoform of human ROMK (Kir1.1b or ROMK2). This isoform was selected for screening as ROMK2 expression extends

along the nephron in both the TAL and CCD. In contrast, ROMK1 is not expressed in the TAL.<sup>7</sup>

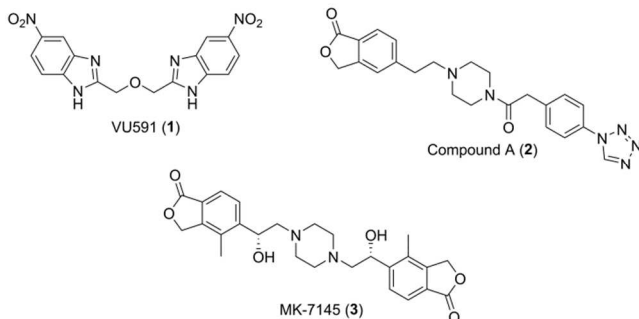


**Figure 1.** Structures of ROMK inhibitors VU591, Compound A, and MK-7145.

This screening campaign led to the identification of 3-sulfamoylbenzamide **4** (Figure 2) as a ROMK inhibitor with modest potency ( $\text{TI}^+$  flux  $\text{IC}_{50}$  = 6.5  $\mu\text{M}$ ). Importantly, compound **4** demonstrated minimal inhibition of the related inward rectifying potassium channels Kir2.1 and Kir4.1 as determined by whole-cell patch-clamp assays using CHO cells stably expressing either Kir2.1 or Kir4.1. Compound **4** also possessed minimal affinity ( $K_i$  > 40  $\mu\text{M}$ ) for the human-ether-a-go-go (hERG) potassium channel (product of the hERG gene; Kv11.1) as determined by displacement of a fluorescently labeled derivative of dofetilide from membrane homogenates of HEK-293 cells stably expressing hERG channels.<sup>25</sup> While **4** showed high apparent clearance in human liver microsomal (HLM) incubations,<sup>26, 27</sup> this selectivity profile coupled with reasonable molecular weight, passive permeability ( $P_{\text{app}}$ )<sup>28</sup> and  $\text{LogD}^{29}$  made **4** an attractive lead for further optimization.

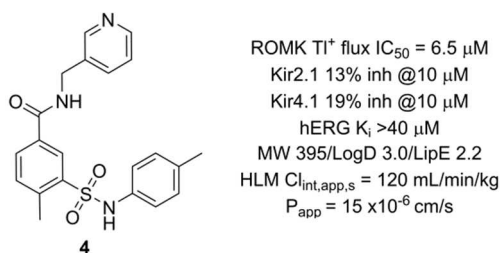


**Figure 2.** Structure and profile of HTS hit **4**.

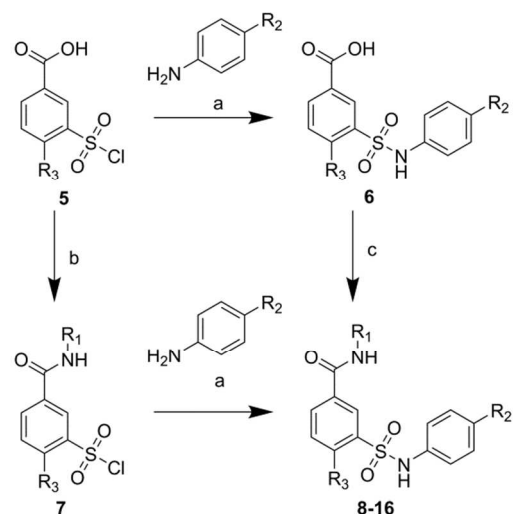
Given the high microsomal turnover and modest potency observed for **4**, we began our optimization efforts with a focus on identifying more potent inhibitors with reduced lipophilicity relative to **4**. The 3-sulfamoylbenzamide scaffold of **4** was amenable to rapid SAR development via both singleton and parallel syntheses starting from 3-(chlorosulfonyl)benzoic acids **5** as illustrated in Scheme 1. The 3-(*N*-arylsulfamoyl)benzoic acids **6** could be accessed by treatment of sulfonyl chlorides **5** with anilines under basic conditions. Subsequent HATU mediated coupling of benzoic acids **6** with amines provided 3-sulfamoylbenzamides. Alternatively, 3-(chlorosulfonyl)benzamides **7** were prepared via amine acylation following activation of 3-(*N*-chlorosulfamoyl)benzoic

acids **5** as the acyl chlorides. Sulfonamide formation under basic conditions then provided 3-sulfamoylbenzamides.

Key results from SAR expansion of this scaffold are presented in Table 1. A scan of the  $\text{R}_1$  amide region provided 3-methyl-1,2,4-oxadiazole **8**, which was 15-fold more potent against ROMK ( $\text{TI}^+$  flux  $\text{IC}_{50}$  = 440 nM) with improved metabolic stability (HLM  $\text{Cl}_{\text{int,app,s}}$  = 30 mL/min/kg) relative to **4**. Compound **8** also showed excellent selectivity over hERG binding ( $K_i$  > 40  $\mu\text{M}$ ) and functional inhibition of the hERG channel in a patch-clamp assay using HEK-293 cells expressing the hERG channel ( $\text{IC}_{50}$  > 100  $\mu\text{M}$ ). While other heterocycles were tolerated in this region (see SI Table 1 for more examples) **8** provided the largest increase in ROMK potency relative to **4** and superior lipophilic efficiency<sup>30</sup> (LipE) compared to other analogues.

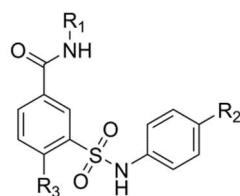
While some tolerance for variation of the  $\text{R}_3$  core benzamide 4-substituent was observed, the presence of this substituent was crucial for good ROMK potency. The 4-unsubstituted benzamide **9** ( $\text{R}_3$  = H) was more than 30-fold less potent ( $\text{TI}^+$  flux  $\text{IC}_{50}$  = 17  $\mu\text{M}$ ;  $n$  = 1) relative to **8**. The 4-methoxy analogue **10** was less potent relative to **8**, but with comparable LipE (3.5 vs. 3.7) and improved metabolic stability (HLM  $\text{Cl}_{\text{int,app,s}}$  = 10 mL/min/kg).

### Scheme 1: Synthetic Routes Used to Prepare 3-Sulfamoylbenzamides 8-16<sup>a</sup>



<sup>a</sup>Reagents and conditions: (a) THF, pyridine, 50-60 °C (40-85% yield); (b)  $\text{SOCl}_2$ , DMF,  $\text{CH}_2\text{Cl}_2$ ; then  $\text{R}_1\text{NH}_2$ , 2,6-lutidine,  $\text{CH}_2\text{Cl}_2$  (40-46% yield); (c)  $\text{R}_1\text{NH}_2$ , HATU,  $i\text{Pr}_2\text{NEt}$ , DMF (22-71% yield)

Although attempts to remove or replace the sulfanilide moiety were not successful, variation of the sulfanilide aromatic ring  $\text{R}_2$  substituent provided a number of compounds with improved ROMK potency and LipE (**11-13**). The *N*-4-(isoxazol-5-yl)phenyl and *N*-4-chlorophenyl sulfonamides **11** and **12** showed ~5-fold improvement in  $\text{TI}^+$  flux potencies ( $\text{IC}_{50}$  = 110 nM and 85 nM, respectively) over **8** but did not offer improved metabolic stability. The *N*-4-(oxazol-5-yl)phenyl analogue **13** showed good ROMK potency ( $\text{TI}^+$  flux  $\text{IC}_{50}$  = 35 nM), but also demonstrated higher turnover in microsomal incubations. Other sulfanilide *para*-substituents were tolerated (see SI Table 1 for more examples), but did not offer the balanced ADME profiles observed for **11-13**.

**Table 1. In Vitro ROMK Potency, hERG Potency, and ADME Properties of Benzamides 8-16**

| Cmpd          | R <sub>1</sub> | R <sub>2</sub>  | R <sub>3</sub>   | hROMK IC <sub>50</sub><br>(μM) <sup>a</sup><br>(pIC <sub>50</sub> ±SD) | HLM Cl <sub>int,app,s</sub><br>(mL/min/kg) <sup>b</sup> | P <sub>app</sub><br>(10 <sup>-6</sup> cm/s) <sup>c</sup> | LogD <sup>d</sup> | LipE | hERG K <sub>i</sub><br>(μM) |
|---------------|----------------|-----------------|------------------|--|---|--|-------------------|------|-----------------------------|
| <b>8</b>      |                | CH <sub>3</sub> | CH <sub>3</sub>  | 0.44<br>(6.4±0.3)  | 30  | 20   | 2.7               | 3.7  | >40                         |
| <b>9</b>      |                | CH <sub>3</sub> | H                | 17 <sup>e</sup>  | 9   | 22   | 2.3               | 2.5  | >40                         |
| <b>10</b>     |                | CH <sub>3</sub> | OCH <sub>3</sub> | 1.3<br>(5.8±0.2)   | 10  | 8  | 2.3               | 3.5  | >40                         |
| <b>11</b>     |                |                 | CH <sub>3</sub>  | 0.11<br>(7.0±0.3)  | 25  | 6  | 2.3               | 4.7  | >40                         |
| <b>12</b>     |                | Cl              | CH <sub>3</sub>  | 0.085<br>(7.0±0.03)  | 35  | 19   | 3.0               | 4.0  | >40                         |
| <b>13</b>     |                |                 | CH <sub>3</sub>  | 0.035<br>(7.5±0.3)   | 69  | 10   | 2.2               | 5.3  | >40                         |
| <b>14</b>     |                |                 | CH <sub>3</sub>  | 0.28<br>(6.6±0.06)   | <8  | 12   | 2.4               | 4.2  | >40                         |
| <b>15</b>     |                | Cl              | CH <sub>3</sub>  | 0.086<br>(7.0±0.09)  | <9  | 19   | 2.9               | 4.1  | >40                         |
| <b>(-)-16</b> |                | Cl              | OCH <sub>3</sub> | 0.16<br>(6.8±0.08)   | <8  | 16   | 2.6               | 4.2  | 28                          |
| <b>(+)-16</b> |                | Cl              | OCH <sub>3</sub> | 13<br>(4.9±0.1)  | <8  | 11   | 2.7               | 2.2  | >40                         |

<sup>a</sup> IC<sub>50</sub> values are reported as geometric means of n ≥ 2 replicates unless otherwise indicated. <sup>b</sup> Scaled apparent intrinsic clearance using scaling method described in Ref. 23. <sup>c</sup> Measured using MDCKII-LE cell line as described in ref. 24. <sup>d</sup> Measured at pH 7.4 using octanol/buffer shake-flask method as described in Ref. 26. <sup>e</sup> Data reported for a single replicate (n = 1).

With these optimized sulfonamides and benzamide cores in place, iterative scanning of the amide R<sub>1</sub> region led to the identification of a series of triazoles (**14-16**) as ROMK inhibitors with well-balanced in vitro metabolic stability, passive permeability and ROMK potency profiles. The ROMK potencies of 1-methyl-1*H*-1,2,3-triazoles **14** (TI<sup>+</sup> flux IC<sub>50</sub> = 280 nM) and **15** (TI<sup>+</sup> flux IC<sub>50</sub> = 86 nM) were similar to those of the oxadiazole **11** and **12**. However, triazoles **14** and **15** were more stable in HLM incubations (HLM Cl<sub>int,app,s</sub> < 8 and < 9 mL/min/kg, respectively) than their oxadiazole comparators. The regioisomeric 2-methyl-2*H*-1,2,3-triazole (-)-**16** (PF-06807656) was also a potent ROMK inhibitor (TI<sup>+</sup> flux IC<sub>50</sub> = 160 nM) with low HLM turnover and good passive permeabil-

ity. The enantiomeric 2-methyl-2*H*-1,2,3-triazole (+)-**16** was 80-fold less potent relative to (-)-**16**. While the more active enantiomer (-)-**16** did demonstrate weak affinity for the hERG channel (K<sub>i</sub> = 28 μM), it maintained the good selectivity for ROMK inhibition over hERG channel binding observed in this series. It should be noted that, in general, introduction of an α-methyl substituent, as found in **16**, led to improved aqueous solubility with minimal impact on ROMK potency.

Based on their attractive *in vitro* ADME profiles, **14** and (-)-**16** were selected for further characterization in whole-cell patch-clamp experiments measuring inhibition of ROMK2 currents. These data (SI Figure 1) confirmed that, as indicated in the TI<sup>+</sup> flux assay, these compounds are potent inhibitors of

human ROMK2. However, it was discovered that they lack inhibitory activity against the rat ROMK2 channel in an analogous patch-clamp assay, a surprising result given the similarity of human and rat ROMK (> 92% identity for ROMK2) and the similar human and rat potencies of previously reported ROMK inhibitors.<sup>11</sup>

The in vitro activity of previously reported ROMK inhibitors has mostly been evaluated using the longer Kir1.1 splice variant, Kir1.1a (ROMK1), which possesses 19 additional amino acids at the N-terminus relative to ROMK2. As shown in Table 2, the inhibitory activity of compounds **12**, **14**, and (–)-**16** was maintained in testing against ROMK1. In a TI<sup>+</sup>-flux assay, compounds **12**, **14**, and (–)-**16** were able to inhibit hROMK1 in a concentration dependent manner. These results were further confirmed using the gold standard patch-clamp electrophysiology technique, with all three compounds showing greater ROMK inhibitory potency in the patch-clamp assay relative to the TI<sup>+</sup>-flux assay. In our experience, the shift in apparent potencies between these assay formats is typical behavior from small molecule ROMK inhibitors. The species disconnect was maintained in testing against the longer Kir1.1 splice variant as well. In the TI<sup>+</sup>-flux assay, known Kir1.1 inhibitor **1** was able to inhibit rat ROMK1 with potency similar to that previously reported for inhibition of human ROMK1 (IC<sub>50</sub> = 420 nM and 240 nM for rat and human ROMK, respectively). However, compounds **12**, **14**, and (–)-**16** did not have any effect at concentrations up to 30 μM (for representative concentration-response curves see SI Figure 2).

**Table 2. In Vitro Rat and Human ROMK1 Potency for Select Inhibitors**

| Cmpd           | hROMK TI <sup>+</sup> flux<br>IC <sub>50</sub> (nM) <sup>a</sup><br>(pIC <sub>50</sub> ±SD) | rROMK TI <sup>+</sup> flux<br>IC <sub>50</sub> (μM) <sup>a</sup><br>(pIC <sub>50</sub> ±SD) | hROMK<br>patch-clamp<br>IC <sub>50</sub> (nM) <sup>b</sup><br>(95% CI) |
|----------------|---|---|--|
| <b>1</b>       | 744<br>(6.1±0.3)  | 0.420<br>(6.4±0.4)  | N.D. <sup>c</sup>  |
| <b>12</b>      | 777<br>(6.1±0.06)   | >30   | 62<br>(61-64)  |
| <b>14</b>      | 1042<br>(5.9±0.3)   | >30   | 104<br>(31-117)  |
| (–)- <b>16</b> | 391<br>(6.4±0.03)   | >30   | 61<br>(63-171)   |

<sup>a</sup> IC<sub>50</sub> values are reported as geometric means of n≥3 replicates unless otherwise indicated. <sup>b</sup> Reported IC<sub>50</sub> values are derived from global fit to a five point concentration-response curve with n≥4 for each concentration. <sup>c</sup> Not Determined.

Based on in silico docking and functional analysis of ROMK mutants, it has been proposed that **1** binds in the ROMK conduction pore at a site ~6.5 Å below the channel selectivity filter in the proximity of N171 and in contact with two adjacent ROMK subunits.<sup>31</sup> Consistent with this model, the ROMK N171D mutant is insensitive to inhibition by **1**. A similar result has been reported for **2**, which inhibits the N171D mutant with ~90-fold lower potency relative to its activity against the wild-type channel.<sup>22</sup> Since N171 has been identified as a conserved part of the small molecule binding site for these previously discovered ROMK inhibitors, we

wanted to test if it also plays a role in the inhibition of the hKir1.1 channel by the novel inhibitors reported herein. As previously shown, the N171D mutation results in a ROMK channel which does not express well unless a second mutation, K80M, is introduced.<sup>32, 33</sup> Thus, these studies were carried out in the K80M background. While the K80M mutation restores the functional expression of N171 mutants it does not affect channel inhibition by (–)-**16** (SI Figure 3). Interestingly mutating asparagine to aspartate at position 171 does not affect the inhibition of ROMK currents by compound (–)-**16** (Figure 3). This behavior is in contrast to that reported for inhibitors **1** and **2**, both of which show markedly lower inhibitory activity against the N171D mutant channel.

In summary, a series of 3-(sulfamoyl)benzamide ROMK inhibitors has been discovered following identification of **4** as a hit from a high-throughput screening campaign of the Pfizer compound collection. Optimization of this series has provided a number of compounds with well-balanced in vitro ADME properties and ROMK inhibitory potency. In contrast to previously reported small-molecule ROMK inhibitors, these compounds lack inhibitory activity at the rat ROMK channel. The inhibitory activity of (–)-**16** is insensitive to the introduction of the N171D mutation in the ROMK conduction pore that greatly diminishes the activity of other small-molecule inhibitors. Taken together, these results suggest that the series of inhibitors described herein interact with ROMK in a mode distinct from previously reported inhibitors. Future work is planned to elucidate the nature of the interaction of ROMK with these inhibitors.

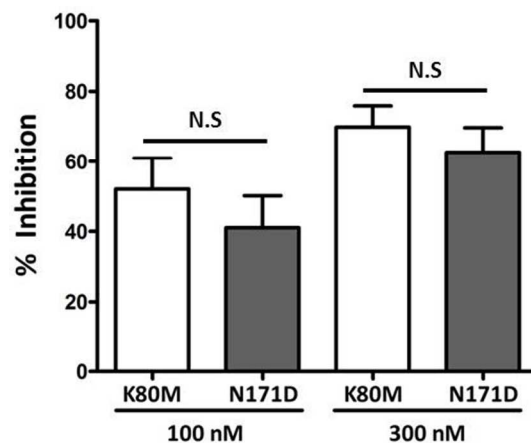


**Figure 3.** Inhibition of human ROMK K80M and K80M/N171D currents by compound (–)-**16**. Whole-cell currents in HEK293 cells transiently expressing human ROMK K80M (open bars) or human ROMK K80M/N171D (dark bars) channels were examined under voltage clamp conditions as described in the Supporting Information. (N.S. = statistically not significant)

## ASSOCIATED CONTENT

### Supporting Information

The Supporting Information is available free of charge on the ACS Publications website.

Details for the synthesis of key intermediates and analytical data for compounds **8-16**; Experimental details for ROMK1 TI<sup>+</sup>-flux

and electrophysiology experiments; Representative  $\text{TI}^+$ -flux concentration-response curves for compounds **1**, **12**, **14**, and (-)-**16**; Effect of ROMK1 K80M mutation on inhibition by (-)-**16**. (PDF)

## AUTHOR INFORMATION

### Corresponding Authors

\* E-mail: [matthew.sammons@pfizer.com](mailto:matthew.sammons@pfizer.com)

\* E-mail: [sujay.v.kharade@vanderbilt.edu](mailto:sujay.v.kharade@vanderbilt.edu)

### Present Addresses

† D.F.: 360 Binney St., Cambridge, MA, 02142, United States.

‡ N.A.C., S.G.Z, and B.M.A.: 4222 Emperor Blvd., Suite 350, Durham, NC, 27703, United States.

### Author Contributions

The manuscript was written through contributions of all authors. All authors have given approval to the final version of the manuscript.

## ACKNOWLEDGMENT

The authors would like to thank James Bradow for SFC resolution and analysis support. We would also like to thank Beth Vetelino and Steve Coffey for synthetic support.

## ABBREVIATIONS

ROMK, renal outer medullary potassium channel; TAL, thick ascending limb of the Loop of Henle; CCD, cortical collecting duct; hERG, human ether-a-go-go gene; HLM, human liver microsomes;  $P_{app}$ , passive permeability; HEK-293, human embryonic kidney 293 cells; CHO, Chinese hamster ovary; DMAP, 4-dimethylaminopyridine; HATU, 1-[bis(dimethylamoni)methylene]-1*H*-1,2,3-triazolo[4,5-*b*]pyridinium-3-oxide hexafluorophosphate; LipE, lipophilic efficiency; ADME, absorption, distribution, metabolism, and excretion; SAR, structure-activity relationship; THF, tetrahydrofuran; DMF, *N,N*-dimethylformamide.

## REFERENCES

- (1) Peacock, W. F.; Costanzo, M. R.; De Marco, T.; Lopatin, M.; Wynne, J.; Mills, R. M.; Emerman, C. L. Impact of Intravenous Loop Diuretics on Outcomes of Patients Hospitalized with Acute Decompensated Heart Failure: Insights from the ADHERE Registry. *Cardiology* **2009**, *113*, 12-19.
- (2) Roush, G. C.; Sica, D. A. Diuretics for Hypertension: A Review and Update. *Am. J. Hypertens.* **2016**, *29*, 1130-1137.
- (3) Kantor, E. D.; Rehm, C. D.; Haas, J. S.; Chan, A. T.; Giovannucci, E. L. Trends in Prescription Drug Use among Adults in the United States from 1999–2012. *JAMA* **2015**, *314*, 1818-1831.
- (4) Palmer, B. F. Metabolic Complications Associated With Use of Diuretics. *Semin. Nephrol.* **2011**, *31*, 542-552.
- (5) De Bruyne, L. K. M. Mechanisms and management of diuretic resistance in congestive heart failure. *Postgrad. Med. J.* **2003**, *79*, 268-271.
- (6) Benjamin, E. J.; Blaha, M. J.; Chiuve, S. E.; Cushman, M.; Das, S. R.; Deo, R.; de Ferranti, S. D.; Floyd, J.; Fornage, M.; Gillespie, C.; Isasi, C. R.; Jiménez, M. C.; Jordan, L. C.; Judd, S. E.; Lackland, D.; Lichtman, J. H.; Lisabeth, L.; Liu, S.; Longenecker, C. T.; Mackey, R. H.; Matsushita, K.; Mozaffarian, D.; Mussolino, M. E.; Nasir, K.; Neumar, R. W.; Palaniappan, L.; Pandey, D. K.; Thiagarajan, R. R.; Reeves, M. J.; Ritchey, M.; Rodriguez, C. J.; Roth, G. A.; Rosamond, W. D.; Sasson, C.; Towfighi, A.; Tsao, C. W.; Turner, M. B.; Virani, S. S.; Voeks, J. H.; Willey, J. Z.; Wilkins, J. T.; Wu, J. H.; Alger, H. M.; Wong, S. S.; Muntner, P. Heart Disease and Stroke Statistics—2017 Update: A Report From the American Heart Association. *Circulation* **2017**.

(7) Welling, P. A.; Ho, K. A comprehensive guide to the ROMK potassium channel: form and function in health and disease. *Am. J. Physiol.: Renal Physiol.* **2009**, *297*, F849-F863.

(8) Denton, J. S.; Pao, A. C.; Maduke, M. Novel diuretic targets. *Am. J. Physiol.: Renal Physiol.* **2013**, *305*, F931-F942.

(9) Kharade, S. V.; Flores, D.; Lindsley, C. W.; Satlin, L. M.; Denton, J. S. ROMK inhibitor actions in the nephron probed with diuretics. *Am. J. Physiol.: Renal Physiol.* **2016**, *310*, F732-F737.

(10) Bhawe, G.; Chauder, B. A.; Liu, W.; Dawson, E. S.; Kadakia, R.; Nguyen, T. T.; Lewis, L. M.; Meiler, J.; Weaver, C. D.; Satlin, L. M.; Lindsley, C. W.; Denton, J. S. Development of a Selective Small-Molecule Inhibitor of Kir1.1, the Renal Outer Medullary Potassium Channel. *Mol. Pharmacol.* **2011**, *79*, 42-50.

(11) Tang, H.; Walsh, S. P.; Yan, Y.; de Jesus, R. K.; Shahripour, A.; Teumelsan, N.; Zhu, Y.; Ha, S.; Owens, K. A.; Thomas-Fowlkes, B. S.; Felix, J. P.; Liu, J.; Kohler, M.; Priest, B. T.; Bailey, T.; Brochu, R.; Alonso-Galicia, M.; Kaczorowski, G. J.; Roy, S.; Yang, L.; Mills, S. G.; Garcia, M. L.; Pasternak, A. Discovery of Selective Small Molecule ROMK Inhibitors as Potential New Mechanism Diuretics. *ACS Med. Chem. Lett.* **2012**, *3*, 367-372.

(12) Tang, H.; de Jesus, R. K.; Walsh, S. P.; Zhu, Y.; Yan, Y.; Priest, B. T.; Swensen, A. M.; Alonso-Galicia, M.; Felix, J. P.; Brochu, R. M.; Bailey, T.; Thomas-Fowlkes, B.; Zhou, X.; Pai, L. Y.; Hampton, C.; Hernandez, M.; Owens, K.; Roy, S.; Kaczorowski, G. J.; Yang, L.; Garcia, M. L.; Pasternak, A. Discovery of a novel subclass of ROMK channel inhibitors typified by 5-(2-(4-(2-(1*H*-Tetrazol-1-yl)phenyl)acetyl)piperazin-1-yl)ethyl)isobenzofuran-1(3*H*)-one. *Bioorg. Med. Chem. Lett.* **2013**, *23*, 5829-5832.

(13) Walsh, S. P.; Shahripour, A.; Tang, H.; Teumelsan, N.; Frie, J.; Zhu, Y.; Priest, B. T.; Swensen, A. M.; Liu, J.; Margulis, M.; Visconti, R.; Weinglass, A.; Felix, J. P.; Brochu, R. M.; Bailey, T.; Thomas-Fowlkes, B.; Alonso-Galicia, M.; Zhou, X.; Pai, L.-Y.; Corona, A.; Hampton, C.; Hernandez, M.; Bentley, R.; Chen, J.; Shah, K.; Metzger, J.; Forrest, M.; Owens, K.; Tong, V.; Ha, S.; Roy, S.; Kaczorowski, G. J.; Yang, L.; Parmee, E.; Garcia, M. L.; Sullivan, K.; Pasternak, A. Discovery of a Potent and Selective ROMK Inhibitor with Pharmacokinetic Properties Suitable for Preclinical Evaluation. *ACS Med. Chem. Lett.* **2015**, *6*, 747-752.

(14) Walsh, S. P.; Shahripour, A.; Tang, H.; de Jesus, R. K.; Teumelsan, N.; Zhu, Y.; Frie, J.; Priest, B. T.; Swensen, A. M.; Alonso-Galicia, M.; Felix, J. P.; Brochu, R. M.; Bailey, T.; Thomas-Fowlkes, B.; Zhou, X.; Pai, L.-Y.; Hampton, C.; Hernandez, M.; Owens, K.; Ehrhart, J.; Roy, S.; Kaczorowski, G. J.; Yang, L.; Garcia, M. L.; Pasternak, A. Differentiation of ROMK potency from hERG potency in the phenacetyl piperazine series through heterocycle incorporation. *Bioorg. Med. Chem. Lett.* **2016**, *26*, 2339-2343.

(15) Zhu, Y.; de Jesus, R. K.; Tang, H.; Walsh, S. P.; Jiang, J.; Gu, X.; Teumelsan, N.; Shahripour, A.; Pio, B.; Ding, F.-X.; Ha, S.; Priest, B. T.; Swensen, A. M.; Alonso-Galicia, M.; Felix, J. P.; Brochu, R. M.; Bailey, T.; Thomas-Fowlkes, B.; Zhou, X.; Pai, L.-Y.; Hampton, C.; Hernandez, M.; Owens, K.; Ehrhart, J.; Roy, S.; Kaczorowski, G. J.; Yang, L.; Parmee, E. R.; Sullivan, K.; Garcia, M. L.; Pasternak, A. Discovery of a potent and selective ROMK inhibitor with improved pharmacokinetic properties based on an octahydropyrazino[2,1-*c*][1,4]oxazine scaffold. *Bioorg. Med. Chem. Lett.* **2016**, *26*, 5695-5702.

(16) Chobanian, H. R.; Guo, Y.; Pio, B.; Tang, H.; Teumelsan, N.; Clements, M.; Frie, J.; Ferguson, R.; Guo, Z.; Thomas-Fowlkes, B. S.; Felix, J. P.; Liu, J.; Kohler, M.; Priest, B.; Hampton, C.; Pai, L.-Y.; Corona, A.; Metzger, J.; Tong, V.; Joshi, E. M.; Xu, L.; Owens, K.; Maloney, K.; Sullivan, K.; Pasternak, A. The design and synthesis of novel spirocyclic heterocyclic sulfone ROMK inhibitors as diuretics. *Bioorg. Med. Chem. Lett.* **2017**, *27*, 1109-1114.

(17) Hampton, C.; Zhou, X.; Priest, B. T.; Pai, L.-Y.; Felix, J. P.; Thomas-Fowlkes, B.; Liu, J.; Kohler, M.; Xiao, J.; Corona, A.; Price, O.; Gill, C.; Shah, K.; Rasa, C.; Tong, V.; Owens, K.; Ormes, J.; Tang, H.; Roy, S.; Sullivan, K. A.; Metzger, J. M.; Alonso-Galicia, M.; Kaczorowski, G. J.; Pasternak, A.; Garcia, M. L. The Renal Outer Medullary Potassium Channel Inhibitor, MK-7145, Lowers Blood Pressure, and Manifests Features of Bartter's Syndrome Type II Phenotype. *J. Pharmacol. Exp. Ther.* **2016**, *359*, 194-206.

(18) Zhou, X.; Forrest, M. J.; Sharif-Rodriguez, W.; Forrest, G.; Szeto, D.; Urosevic-Price, O.; Zhu, Y.; Stevenson, A. S.; Zhou, Y.; Stribling, S.; Dajee, M.; Walsh, S. P.; Pasternak, A.; Sullivan, K. A. Chronic Inhibition of Renal Outer Medullary Potassium Channel Not Only Prevented but Also Reversed Development of Hypertension and End-Organ Damage in Dahl Salt-Sensitive Rats. *Hypertension* **2016**.

(19) Dong, S.; VanGelder, K.; Shi, Z.-C.; Yu, Y.; Wu, Z.; Ferguson, R.; Guo, Z. Z.; Tang, H.; Frie, J.; Fu, Q.; Gu, X.; Priest, B. T.; Thomas-Fowlkes, B.; Weinglass, A.; Margulis, M.; Liu, J.; Pai, L.-Y.; Hampton, C.; Haimbach, R. E.; Owens, K.; Tong, V.; Xu, S.; Hu, M.; Zingaro, G. J.; Morissette, P.; Ehrhart, J.; Roy, S.; Sullivan, K.; Pasternak, A. Improvement of hERG-ROMK index of spirocyclic ROMK inhibitors through scaffold optimization and incorporation of novel pharmacophores. *Bioorg. Med. Chem. Lett.* **2017**, *27*, 2559-2566.

(20) Tang, H.; Zhu, Y.; Teumelsan, N.; Walsh, S. P.; Shahripour, A.; Priest, B. T.; Swensen, A. M.; Felix, J. P.; Brochu, R. M.; Bailey, T.; Thomas-Fowlkes, B.; Pai, L.-Y.; Hampton, C.; Corona, A.; Hernandez, M.; Metzger, J.; Forrest, M.; Zhou, X.; Owens, K.; Tong, V.; Parmee, E.; Roy, S.; Kaczorowski, G. J.; Yang, L.; Alonso-Galicia, M.; Garcia, M. L.; Pasternak, A. Discovery of MK-7145, an Oral Small Molecule ROMK Inhibitor for the Treatment of Hypertension and Heart Failure. *ACS Med. Chem. Lett.* **2016**, *7*, 697-701.

(21) Pasternak, A. Discovery of ROMK Inhibitor MK-7145: A Novel Mechanism Diuretic. In *Comprehensive Medicinal Chemistry III*, Rotella, D., Ward, S.E., Eds.; Elsevier: Oxford, 2017; pp 308-338.

(22) Garcia, M. L.; Priest, B. T.; Alonso-Galicia, M.; Zhou, X.; Felix, J. P.; Brochu, R. M.; Bailey, T.; Thomas-Fowlkes, B.; Liu, J.; Swensen, A.; Pai, L. Y.; Xiao, J.; Hernandez, M.; Hoagland, K.; Owens, K.; Tang, H.; de Jesus, R. K.; Roy, S.; Kaczorowski, G. J.; Pasternak, A. Pharmacologic inhibition of the renal outer medullary potassium channel causes diuresis and natriuresis in the absence of kaliuresis. *J. Pharmacol. Exp. Ther.* **2014**, *348*, 153-164.

(23) Martelli, A.; Testai, L.; Breschi, M. C.; Calderone, V. Inhibitors of the renal outer medullary potassium channel: a patent review. *Expert Opin. Ther. Pat.* **2015**, *25*, 1035-1051.

(24) Yu, H.-b.; Li, M.; Wang, W.-p.; Wang, X.-l. High throughput screening technologies for ion channels. *Acta Pharmacol. Sin.* **2016**, *37*, 34-43.

(25) Deacon, M.; Singleton, D.; Szalkai, N.; Pasieczny, R.; Peacock, C.; Price, D.; Boyd, J.; Boyd, H.; Steidl-Nichols, J. V.; Williams, C. Early evaluation of compound QT prolongation effects: A

predictive 384-well fluorescence polarization binding assay for measuring hERG blockade. *J. Pharmacol. Toxicol. Methods* **2007**, *55*, 255-264.

(26) Obach, R. S. The prediction of human clearance from hepatic microsomal metabolism data. *Curr. Opin. Drug Discovery Dev.* **2001**, *4*, 36-44.

(27) Obach, R. S.; Baxter, J. G.; Liston, T. E.; Silber, B. M.; Jones, B. C.; Macintyre, F.; Rance, D. J.; Wastall, P. The Prediction of Human Pharmacokinetic Parameters from Preclinical and *In Vitro* Metabolism Data. *J. Pharmacol. Exp. Ther.* **1997**, *283*, 46-58.

(28) Di, L.; Whitney-Pickett, C.; Umland, J. P.; Zhang, H.; Zhang, X.; Gebhard, D. F.; Lai, Y.; Federico Iii, J. J.; Davidson, R. E.; Smith, R.; Reyner, E. L.; Lee, C.; Feng, B.; Rotter, C.; Varma, M. V.; Kempshall, S.; Fenner, K.; El-kattan, A. F.; Liston, T. E.; Troutman, M. D. Development of a new permeability assay using low-efflux MDCKII cells. *J. Pharm. Sci.* **2011**, *100*, 4974-4985.

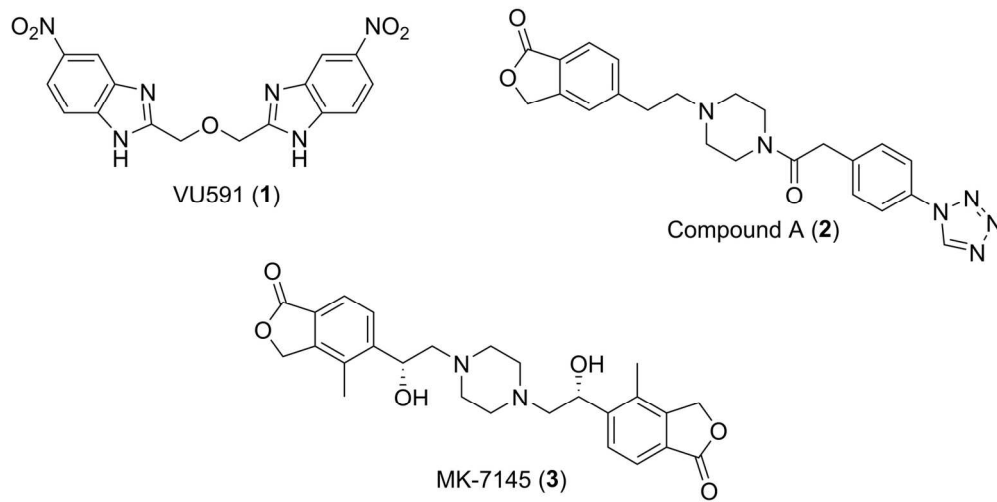
(29) Hay, T.; Jones, R.; Beaumont, K.; Kemp, M. Modulation of the Partition Coefficient between Octanol and Buffer at pH 7.4 and pK<sub>a</sub> to Achieve the Optimum Balance of Blood Clearance and Volume of Distribution for a Series of Tetrahydropyran Histamine Type 3 Receptor Antagonists. *Drug Metab. Disp.* **2009**, *37*, 1864-1870.

(30) Ryckmans, T.; Edwards, M. P.; Horne, V. A.; Correia, A. M.; Owen, D. R.; Thompson, L. R.; Tran, I.; Tutt, M. F.; Young, T. Rapid assessment of a novel series of selective CB2 agonists using parallel synthesis protocols: A Lipophilic Efficiency (LipE) analysis. *Bioorg. Med. Chem. Lett.* **2009**, *19*, 4406-4409.

(31) Swale, Daniel R.; Sheehan, Jonathan H.; Banerjee, S.; Husni, Afeef S.; Nguyen, Thuy T.; Meiler, J.; Denton, Jerod S. Computational and Functional Analyses of a Small-Molecule Binding Site in ROMK. *Biophys. J.* **2015**, *108*, 1094-1103.

(32) Fallen, K.; Banerjee, S.; Sheehan, J.; Addison, D.; Lewis, L. M.; Meiler, J.; Denton, J. S. The Kir channel immunoglobulin domain is essential for Kir1.1 (ROMK) thermodynamic stability, trafficking and gating. *Channels* **2009**, *3*, 57-68.

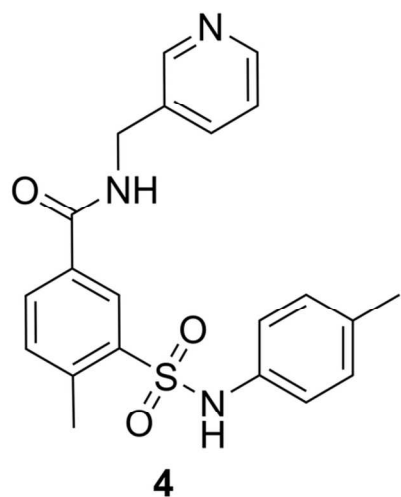
(33) Schulte, U.; Hahn, H.; Konrad, M.; Jeck, N.; Derst, C.; Wild, K.; Weidemann, S.; Ruppertsberg, J. P.; Fakler, B.; Ludwig, J. pH gating of ROMK (Kir1.1) channels: Control by an Arg-Lys-Arg triad disrupted in antenatal Bartter syndrome. *Proc. Natl. Acad. Sci. U.S.A.* **1999**, *96*, 15298-15303.



23  
24  
25  
26  
27  
28  
29  
30  
31  
32  
33  
34  
35  
36  
37  
38  
39  
40  
41  
42  
43  
44  
45  
46  
47  
48  
49  
50  
51  
52  
53  
54  
55  
56  
57  
58  
59  
60

Figure 1. Structures of ROMK inhibitors VU591, Compound A, and MK-7145.

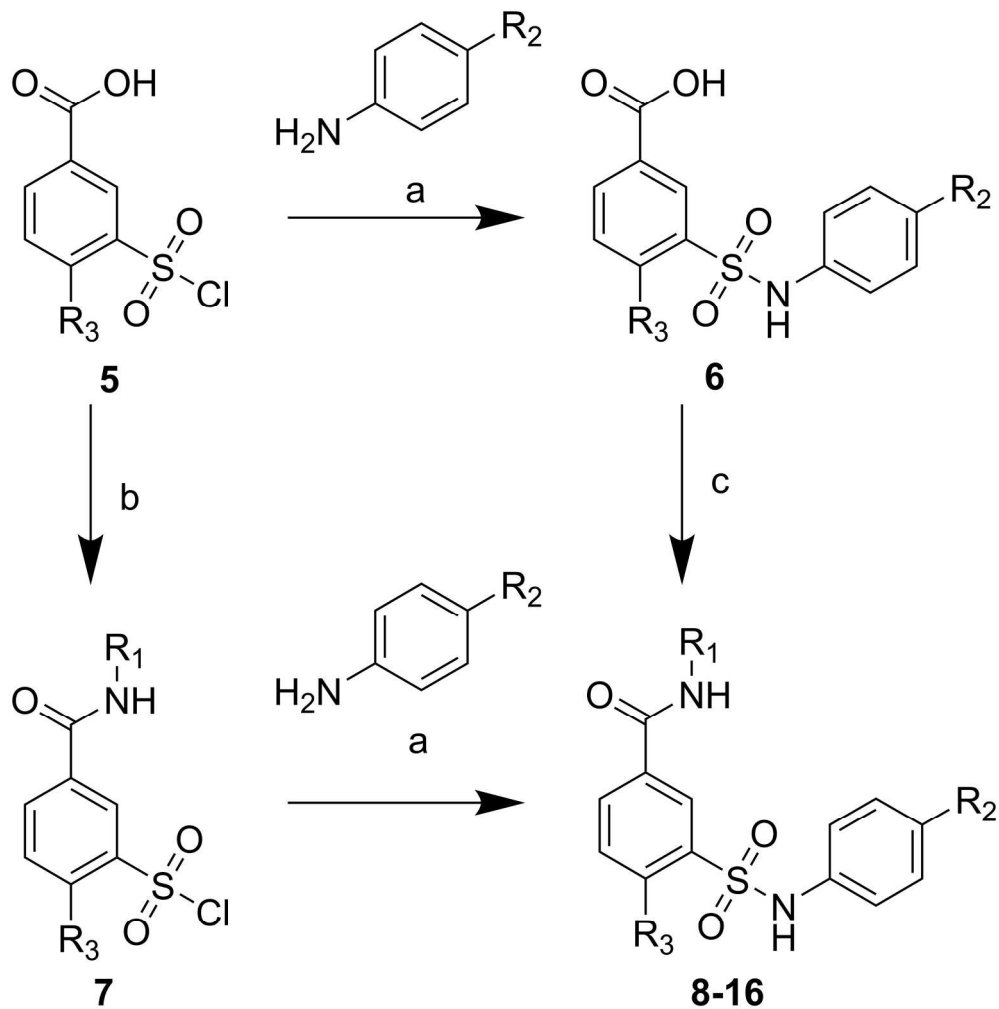
75x38mm (600 x 600 DPI)



ROMK  $\text{TI}^+$  flux  $\text{IC}_{50} = 6.5 \mu\text{M}$   
Kir2.1 13% inh @10  $\mu\text{M}$   
Kir4.1 19% inh @10  $\mu\text{M}$   
hERG  $\text{K}_i >40 \mu\text{M}$   
MW 395/LogD 3.0/LipE 2.2  
HLM  $\text{Cl}_{\text{int,app,s}} = 120 \text{ mL/min/kg}$   
 $\text{P}_{\text{app}} = 15 \times 10^{-6} \text{ cm/s}$

Figure 2. Structure and profile of HTS hit 4.

48x24mm (600 x 600 DPI)



Scheme 1: Synthetic Routes Used to Prepare 3-Sulfamoylbenzamides 8-16a

97x99mm (600 x 600 DPI)

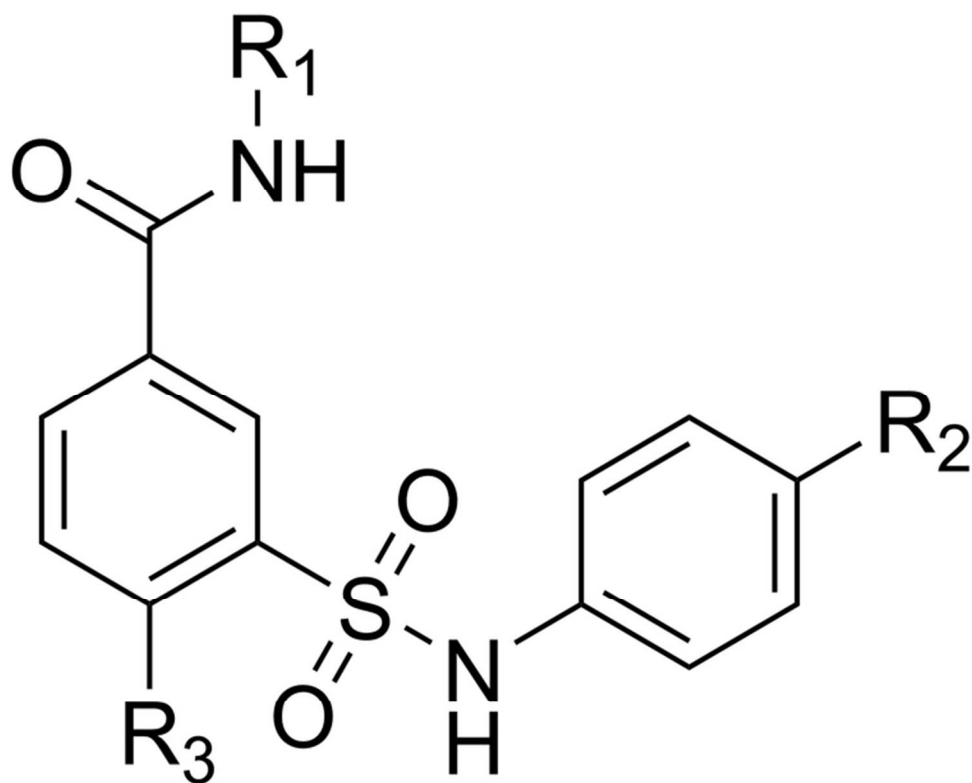


Table 1. In Vitro ROMK Potency, hERG Potency, and ADME Properties of Benzamides 8-17

33x26mm (600 x 600 DPI)

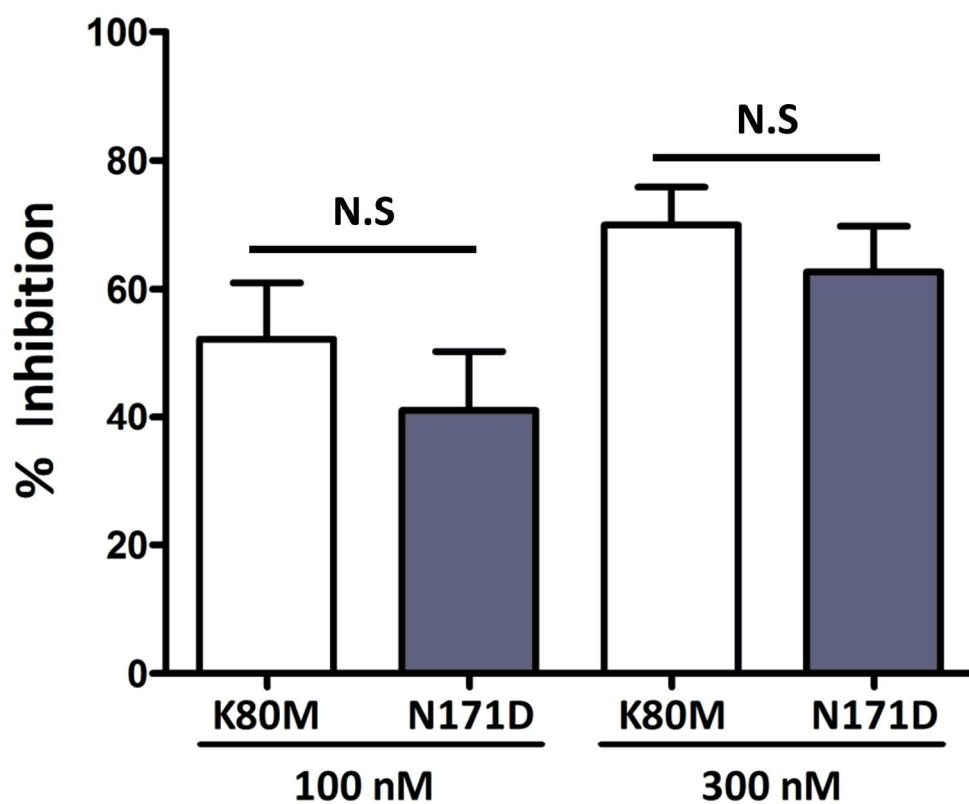
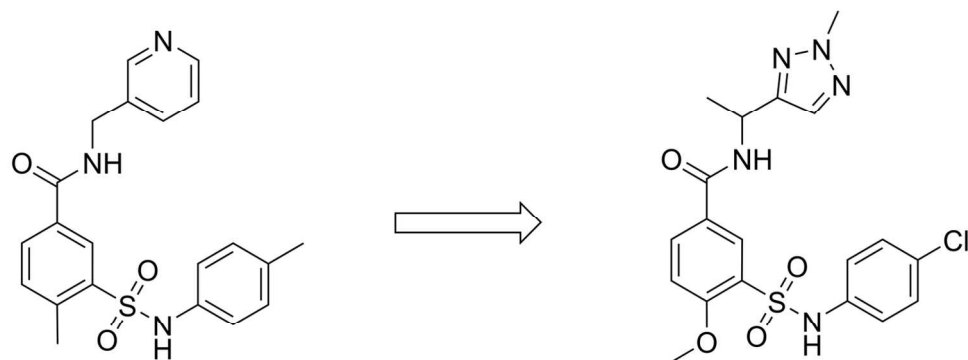


Figure 3. Inhibition of human ROMK K80M and K80M/N171D currents by compound (-)-16. Whole-cell currents in HEK293 cells transiently expressing human ROMK K80M (open bars) or human ROMK K80M/N171D (dark bars) channels were examined under voltage clamp conditions as described in the Supporting Information. (N.S = statistically not significant)

93x79mm (600 x 600 DPI)



**HTS hit 4**  
ROMK  $\text{Ti}^+$  flux  $\text{IC}_{50}$  = 6.5  $\mu\text{M}$

**(-)-16 (PF-06807656)**  
ROMK  $\text{Ti}^+$  flux  $\text{IC}_{50}$  = 160 nM  
ROMK patch-clamp  $\text{IC}_{50}$  = 61 nM

65x34mm (600 x 600 DPI)